Chemistry–A European Journal
Research Article
doi.org/10.1002/chem.202203206
Chemistry Europe
European Chemical Societies Publishing
www.chemeurj.org

Three- and Five-Membered Anionic Chains of Pnictogenylboranes

Mehdi Elsayed Moussa[+],[a] Tobias Kahoun[+],[a] Christian Marquardt,[a] Matthias T. Ackermann,[a] Oliver Hegen,[a] Michael Seidl,[a] Alexey Y. Timoshkin,[b] Alexander V. Virovets,[a] Michael Bodensteiner,[a] and Manfred Scheer*[a]

Dedicated to Professor Dietrich Gudat on the occasion of his 65th birthday.

Abstract: An unprecedented family of three- and five-membered substituted anionic derivatives of parent pnictogenylboranes is herein reported. Reacting various combinations of the pnictogenylboranes $H_2E'–BH_2–NMe_3$ (E′ = P, As) with pnictogen-based nucleophiles MER1R2 (E = P, As; R1 = H, R2 = ^{t}Bu; R1 = R2 = Ph; M = Na, K) allows for the isolation of the unsymmetrical products [Na(18-crown-6)][$H_2E'–BH_2–EH^tBu$] (**3**: E = E′ = P; **4**: E = E′ = As; **5**: E = As, E′ = P) and [M(C)][$H_2E'–BH_2–EPh_2$] (**7**: E = E′ = P, M = Na, C = 18-crown-6; **8**: E = E′ = As; M = K, C = [2.2.2]cryptand; **9**: E = P, E′ = As, M = Na, C = [2.2.2]cryptand; **10**: E = As, E′ = P, M = K, C = [2.2.2]cryptand). [Na(18-crown-6)][$H_2As–BH_2$-^{t}BuPH–BH_3] (**6**) is only accessible by a different pathway, using ^{t}BuPH_2, $BH_3 \cdot SMe_2$ and $NaNH_2$ as starting materials. Additionally, the synthesis of symmetrical diphenyl-substituted compounds [M(18-crown-6)][$Ph_2E–BH_2–EPh_2$] (**11**: E = P, M = Na; **12**: E = As, M = K) is reported which can be regarded as isostructural inorganic, negatively charged analogs of dppm (1,1-bis(diphenylphosphino)methane) and dpam (1,1-bis(diphenylarsino)methane). Furthermore, an elongation of the pnictogen boron backbone in compounds **3**, **7** and **9**′ (similar compound to **9**, stabilized however by 18-crown-6), is attainable by reacting them with the pnictogenylboranes $H_2E'–BH_2–NMe_3$ leading to corresponding five-membered chain-like compounds [Na(18-crown-6)][$H_2E–BH_2–R1R2P–BH_2–E'H_2$] (E = E′ = P, R1 = H, R2 = ^{t}Bu (**13**); E = E′ = P, R1 = R2 = Ph (**14**); E = E′ = As, R1 = R2 = Ph (**15**); E = P, E′ = As, R1 = R2 = Ph (**16**)). Finally, the thermodynamics of the reaction pathways were evaluated by quantum chemical computations.

Introduction

During the last two decades, phosphine-borane derivatives have witnessed significant progress due to their facile accessibility, high modularity and fascinating reactivity.[1,2] Besides being common in synthetic and stereochemical studies,[2] they have been used as precursors/catalysts in hydroboration[3] and hydrophosphination[4] reactions. Moreover, these compounds exhibit potential as cell-permeable drugs[5] and in the activation and transfer of H_2 and other small molecules.[6] With the P–B bonds being isoelectronic to C–C single bonds, poly(phosphine-boranes) with P–B backbones are viewed as an alternative class of inorganic analogs to organic polymers such as polyolefins, possessing, however, significantly different properties.[7] These compounds are commonly obtained via metal-catalyzed dehydrocoupling processes of the corresponding phosphine-borane monomers $RH_2P \cdot BH_3$ (R = alkyl, aryl).[8] Recently, an expansion of improved catalytic[7a,b,9] and non-catalytic[10] procedures was achieved. This progress allowed for enlarging the library of high molar mass polyphosphinoboranes and, to some extent, for the control over their molar mass paving the path for further investigation directions in this research area. In this field, our group is actively involved in the synthesis and reactivity of Lewis base-stabilized pnictogenylboranes $R_2E–BH_2 \cdot NMe_3$ (E = P, As; R = H, alkyl, aryl).[11] The coordination behavior of these compounds towards coinage metal salts,[12] their oxidation with chalcogens[13] and their use as building blocks for the synthesis of oligomeric[14] and polymeric compounds[15] were investigated. Not long ago, we synthesized the first hydrogen- and *tert*-butyl-substituted anionic pnictogenylboranes [M-($C_{12}H_{24}O_6$)][$H_2E–BH_2–EH_2$] (E = P, As; M = Na, K), [Na($C_{12}H_{24}O_6$)][$H_2As–BH_2–PH_2–BH_2–AsH_2$][16] and [Na($C_{12}H_{24}O_6$)(THF)$_2$][^{t}BuHE–$BH_2$–E$H^t$Bu] (E = P, As)[17] and studied

[a] Dr. M. E. Moussa,[+] Dr. T. Kahoun,[+] Dr. C. Marquardt, Dr. M. T. Ackermann, Dr. O. Hegen, Dr. M. Seidl, Dr. A. V. Virovets, Dr. M. Bodensteiner, Prof. Dr. M. Scheer
Institut für Anorganische Chemie der Universität Regensburg
93040 Regensburg (Germany)
E-mail: manfred.scheer@chemie.uni-regensburg.de
Homepage: https://www.uni-regensburg.de/chemie-pharmazie/anorganische-chemie-scheer

[b] Prof. Dr. A. Y. Timoshkin
Institute of Chemistry
St. Petersburg State University
Universitetskaya nab. 7/9, 199034, St. Petersburg (Russia)

[+] These authors contributed equally to this work.

Supporting information for this article is available on the WWW under https://doi.org/10.1002/chem.202203206

their coordination chemistry towards tungsten and copper metal salts. These reactions allowed for the formation of unprecedented metallacycles and 3D inorganic MOF-like aggregates.[17] Based on these results, in addition to a reported investigation on enriching the versatility of phosphine-boron properties by introducing a variety of substituents on phosphorus and boron,[18] we were increasingly motivated to enlarge the library of anionic pnictogenylboranes which will consequently open the door to their future use as building units in the construction of supramolecular aggregates with unique properties. Herein we report on the synthesis and characterization of novel unsymmetrical anionic three-membered substituted pnictogenylboranes in addition to unique five-membered anionic chain-like compounds containing terminal parent phosphine and arsine groups. Further, a synthetic route to inorganic, anionic dppm (1,1-bis(diphenylphosphino)methane) and dpam (1,1-bis(diphenylarsino)methane) analogs is presented.

Results and Discussion

The reaction of pnictogenylboranes $H_2E{-}BH_2{\cdot}NMe_3$ (E = P (**2a**), As(**2b**)) with organosubstituted pnictogenides **1a**–**1d** allows the synthesis of the unsymmetrical three-membered pnictogenylborane derivatives **3**–**5** and **7**–**10** depending on the starting materials involved in the reactions (Scheme 1, paths **A** and **C**). The formed products can be crystallized only upon the addition of stoichiometric equivalents of 18-crown-6 ($C_{12}H_{24}O_6$ = C1; **3**–**5**, **7**, **11**, **12**) or [2.2.2]cryptand ($C_{18}H_{36}N_2O_6$ = C2; **8**–**10**) to the reaction solutions. Sonication of Na^{t}BuPH (**1a**) with $H_2P{-}BH_2{-}NMe_3$ (**2a**) leads to the formation of the corresponding product Na[$H_2P{-}BH_2{-}^t$BuPH]. After addition of equimolar amounts of 18-crown-6, [Na(C1)][$H_2P{-}BH_2{-}^t$BuPH] (**3**) can be isolated. The analog arsenic-based [Na(C1)][$H_2As{-}BH_2{-}^t$BuAsH] (**4**) and the mixed [Na(C1)][$H_2P{-}BH_2{-}^t$BuAsH] (**5**) compounds are accessible by the reaction of **1b** with **2b** and **2a** respectively, at room temperature. The reaction of Na^{t}BuPH (**1a**) with $H_2As{-}BH_2{-}NMe_3$ (**2b**) however, does not work similarly leading to the expected product Na[$H_2As{-}BH_2{-}^t$BuPH]. Instead, the formation of ^{t}BuPH$_2$ and the decomposition of $H_2As{-}BH_2{-}NMe_3$ (**2b**) were observed. Nevertheless, it is possible to obtain compound **6** [Na(C1)][$H_2As{-}BH_2{-}^t$BuPH$-BH_3$] from the reaction of the nucleophile Na[^{t}BuPH$-BH_3$] with $H_2As{-}BH_2{-}NMe_3$ (**2b**) after addition of equimolar amounts of 18-crown-6 (Scheme 1, path **B**). The nucleophile Na[^{t}BuPH$-BH_3$] is accessible by the coordination of BH_3 towards ^{t}BuPH$_2$ using BH_3-SMe_2 and subsequent metalation with $NaNH_2$.[19]

Compounds [Na(C1)][$H_2P{-}BH_2{-}PPh_2$] (**7**) and [Na(C2)][$H_2As{-}BH_2{-}PPh_2$] (**9**) are obtained by performing the reactions at room temperature, while [K(C2)][$H_2As{-}BH_2{-}AsPh_2$] (**8**) and [K(C2)][$H_2P{-}BH_2{-}AsPh_2$] (**10**) are only accessible by the reaction of the corresponding starting materials at 60 °C (**8**) and 70 °C (**10**), respectively (Scheme 1, path **C,** for further information see Supporting Information). Compound **7** is obtained by sonicating a solution of $H_2P{-}BH_2{-}NMe_3$ (**2a**) with $NaPPh_2$ (**1c**), followed by the addition of 18-crown-6 to the reaction solution. However, compounds **8**–**10** can be isolated from the reactions of **1d** + **2b** (**8**), **1c** + **2b** (**9**) and **1d** + **2a** (**10**) as crystalline compounds only after the addition of [2.2.2]cryptand to their reaction solutions, because adding 18-crown-6 instead results in the formation of oily products which limits their characterizations to only solution studies (Scheme 1).

The addition of diphenyl-pnictogenylboranes $Ph2E{-}BH_2{-}NMe_3$ (E=P, As) to diphenyl-substituted pnictogen-based nucleophiles $MEPh_2$ (**1c**, E = P, M = Na; **1d**, E = As, M = K) does not allow any reaction even though various reaction conditions were tested. Rather, the addition of $IBH_2{-}SMe_2$ to a solution of **1c** and **1d** at −80 °C using a 2:1 stochiometric ratio allowing the reaction mixture to react at room temperature leads to the symmetrical three-membered products Na[$Ph_2P{-}BH_2{-}PPh_2$] and K[$Ph_2As{-}BH_2{-}AsPh_2$], respectively. The addition of equimolar amounts of 18-crown-6 to the reaction

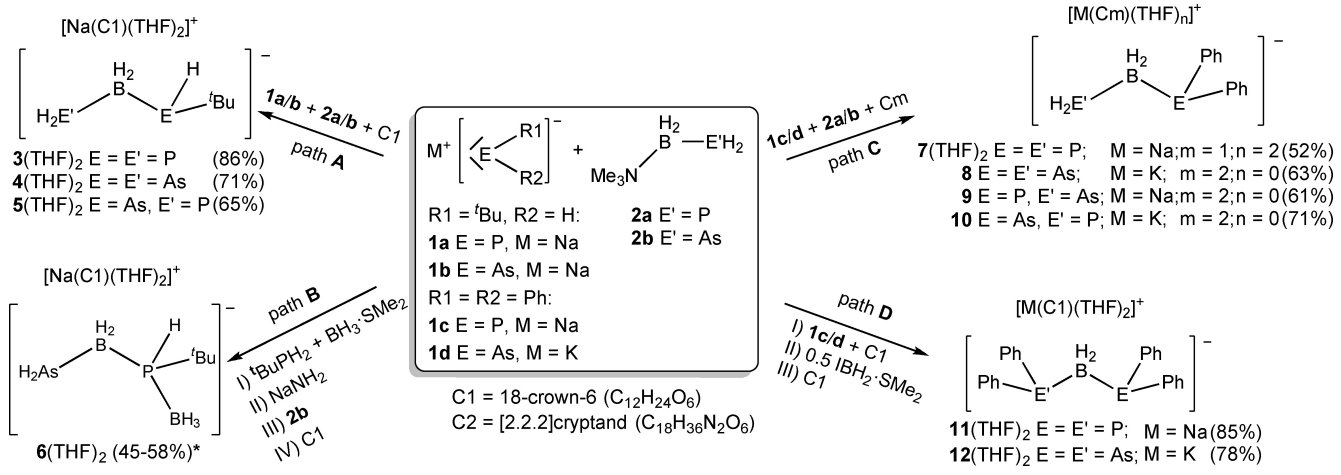

Scheme 1. Synthesis of unsymmetrical path (**A**–**C**) and symmetrical path (**D**) anionic pnictogenylborane chain compounds; Yields are given in parentheses. *variable content of THF.

solutions results in the formation of products **11** and **12** (Scheme 1, path **D**).

According to heteronuclear NMR spectroscopy of the crude reaction solutions, compounds **4**, **8**, **9**, **10** and **12** are selectively obtained from the reactions of their corresponding starting materials. In the crude reaction mixture of compound **6**, the additional formation of the anionic species $[H_3B–^tBuPH–BH_3]^-$ can be observed. During the synthesis of compounds **5** and **11**, signals related to minor impurities can be detected. Nonetheless, all compounds **3**–**12** could be smoothly isolated as pure crystalline materials after crystallization in reasonable yields and investigated by heteronuclear NMR spectroscopy summarized in Table 1.[20] In the ^{31}P NMR spectra of the *tert*-butyl-substituted compounds **3** and **5**, it is observed that the signals associated to the PH_2 groups are slightly upfield shifted ($\delta = -188.8$ ppm (**3**); $\delta = -189.3$ ppm (**5**)) compared to that of the parent compound ($[H_2P–BH_2–PH_2]^-$, $\delta = -175.0$ ppm). This shift is more distinct for the diphenyl-substituted compounds **7** ($\delta = -203.3$ ppm) and **10** ($\delta = -202.9$ ppm). The ^{11}B NMR spectra of the derivatives **3**–**5** and **7**–**10** display signals which are downfield shifted ($\delta = -33.8$ (**3**), −32.6 (**4**), −32.9 (**5**), −29.1 (**7**), −28.0 (**8**), −28.9 (**9**) and −28.0 (**10**) ppm) compared to those of the parent compounds ($[H_2E–BH_2–EH_2]^-$, $\delta = -34.7$ (E = P), −34.5 (E = As) ppm). Clearly, these shifts are more pronounced in the case of the diphenyl-substituted derivatives **7**–**10** in comparison to those of the *tert*-butyl-substituted compounds **3**–**5**. For compound **6**, the shift is reversed to the observed trend, in this case, the signal of the BH_2 group appears at −36.6 ppm. For all compounds **3**–**12**, the $^1J_{B,H}$ coupling constants are similar to the values reported for the parent compounds $[H_2E–BH_2–EH_2]^-$ (E = P, As). Notably, the values of the $^1J_{P,H}$ and $^1J_{B,P}$ coupling constants of **6** are larger compared to the other compounds as well as the parent compounds. This deviation can be explained by the coordination of the additional BH_3 group on the P atom in **6**. In the room temperature ^1H NMR spectra of **7** and **10**, the signals attributed to the terminal PH_2 moieties occur each as a broad doublet ($^1J_{H,P} = 173$ Hz (**7**), 174 Hz (**10**)). Such signals appear as two sets of multiplets in each of the ^1H NMR spectra of **3** and **5**. This effect is caused by the chiral center located at the *tert*-butyl-substituted pnictogen atom in **3** and **5**, indicating the presence of two isomers. The signals of the terminal AsH_2 groups in the compounds **4**, **6**, **8** and **9** occur as multiplets in a slightly negative ppm range (−0.16 ppm (**4**), −0.08 ppm (**6**), −0.23 ppm (**8**), −0.26 ppm (**9**)), indicating the hydridic character of the hydrogen atoms (for further information see Supporting Information).

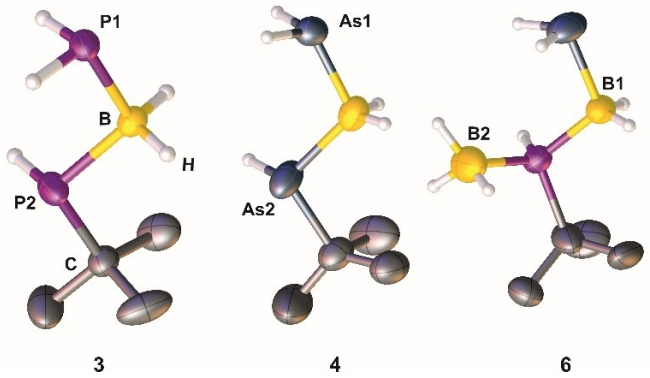

Figure 1. Molecular structures of the anions in **3**, **4** and **6**. Hydrogen atoms bonded to carbon atoms as well as cations are omitted for clarity. Thermal ellipsoids are drawn with 50% probability. Only the major part of the disorder is depicted.

All compounds can be isolated in the solid state as crystalline materials by storing the corresponding saturated THF-solutions layered with *n*-hexane (**3**, **4**, **5**, **6**) or diethyl ether (**8**, **9**, **10**, **11**, **12**) or storing a saturated THF/*n*-hexane solution (**7**) at −28 °C. Single crystals suitable for X-ray structure analysis could be obtained for compounds **3**, **4**, **6**, **7**, **9**, **11** and **12** (Figures 1 and 2.[22]

Compounds **3**, **4** and **6** crystalize in the centrosymmetric space group $P\bar{1}$. Their solid-state structures show in each case the presence of a disorder revealing two isomers (Figure 1). The bond lengths between the BH_2 groups and the terminal pnictogen atoms in **3**, **4** and **6** are found to be similar ranging between 1.972(2) and 2.076(3) Å. These values are slightly longer than those reported for the parent compounds ($[H_2P–BH_2–PH_2]^-$; 1.960(3) and 1.963(3) Å) and ($[H_2As–BH_2–AsH_2]^-$; 2.062(2) and 2.069(2) Å).[16] In contrast, the B–E bonds (E = central pnictogen atom) vary over a wide range between 1.919(5) and 2.124(9) Å. The E′–B–E angles in **3**, **4** and **6** are in the range 108.88(2)–112.44(2)° which are similar to those of the parent compounds ($[H_2E–BH_2–EH_2]^-$; 109.47(2)–

Table 1. NMR data of compounds **3**–**12** and $[H_2E–BH_2–EH_2]^-$ (E = P, As).[16]

Compound	$\delta(^{31}P)$ P^aH_2 [ppm]	$\delta(^{31}P)$ P^bR1R2 [ppm]	$^1J_{P,H}$ $^{a/b}$ [Hz]	$\delta(^{11}B)$ BH_2 [ppm]	$\delta(^{11}B)$ BH_3 [ppm]	$^1J_{B,H}$ [Hz]	$^1J_{B,P}$ $^{a/b}$ [Hz]
$[H_2P–BH_2–PH_2]^-$	−175.0	–	172.0	−34.7	–	99	26
$[H_2As–BH_2–AsH_2]^-$	–	–	–	−34.5	–	106	–
3	−188.8	−32.9	173/177	−33.8	–	97	27
4	–	–	–	−32.6	–	105	–
5	−189.3	–	174/–	−32.9	–	100	26
6	–	5.7	–/302	−36.6	−40.5	93, 102	56/ 69
7	−203.3	−15.2	173/–	−29.1	–	98	–
8	–	–	–	−28.0	–	106	–
9	–	−16.7	–	−28.9	–	100	–
10	−202.9	–	174/–	−28.0	–	99	23
11	–	−27.7	–	−21.1	–	95	–
12	–	–	–	−19.6	–	102	–

110.99(2)°)[16] but larger than those of the substituted derivatives ([^{t}BuEH–BH_2–^{t}BuEH]$^-$ (E = P, As); 100.2(3)–107.9(6)°).[17]

In **7**, the P2–B bond length (1.973(2) Å) is similar to that found in **3** and slightly elongated compared to that found in [H_2P–BH_2–PH_2]$^-$. The Ph_2P–BH_2 bond lengths in compounds **7** (1.964(2) Å) and **11** (1.976(3)–1.983(3) Å) are only slightly longer compared to those reported for Ph_2P–BH_2–NMe_3 (1.975(2) Å).[10b] The E–B–E angle in **7** (111.39(8)°) is slightly larger than those of the parent compounds [H_2E–BH_2–EH_2]$^-$ (109.47(1)–110.99(2)°).[16] For **11**, the P–B–P angle (118.3(1)°) is even wider than that in [H_2P–BH_2–PH_2]$^-$ (110.4(1)°), however, in **12**, the As–B–As angles (106.6(6)–107.2(2)°) are slightly smaller than those in [H_2As–BH_2–AsH_2]$^-$ (109.47(2)–110.99(2)°).

In the solid-state structures of the compounds **3**, **4**, **7**, **9**, **11** and **12** for the BH_2–ER1R2 fragments, a synclinal arrangement of the pnictogen atom lone pair and the backbone of the molecule can be observed (Figures 1 and 2 >).[23] Also in **6**, where the lone pair of the phosphorus atom coordinates a BH_3 group, a staggered conformation is found. For **3**–**4**, **6** and **7**, an antiperiplanar arrangement of the pnictogen atom lone pair and backbone of the molecule in the EH_2–BH_2 moiety is observed, while the solid-state structure of **9** reveals a synclinal conformation instead.

DFT computations were performed at the B3LYP/6-311 + < C + G** level of theory. Due to large computational costs, the bulky counterions $MC1^+$ and $MC2^+$ were omitted for the computations and only the reactions with anionic counterparts were computed in the gas phase. For all [E′H_2BH_2EH(^{t}Bu)]$^-$ compounds, the conformer in which the E′BEC atoms in the chain are approximately on the same plane are lowest in energy for all considered E, E′-containing compounds. The isomer [AsH_2BH_2PH(^{t}Bu)]$^-$ is more stable than [PH_2BH_2AsH(^{t}Bu)]$^-$ with an energy difference of only 2.1 kJ mol^{-1}. Upon complex formation with BH_3, the difference in energy between [PH_2BH_2AsH(^{t}Bu)·BH_3]$^-$ and [AsH_2BH_2PH(^{t}Bu)·BH_3]$^-$ isomers increases to 28.2 kJ mol^{-1} in favor of the latter, due to stronger donor ability of the phosphorus atom as compared to arsenic. Thermodynamic characteristics for the reaction pathways **A**–**C** (see Supporting Information for details) reveal that all these reaction pathways are exothermic and exergonic in the gas phase at room temperature for all considered compounds, which indicates that the practical difficulties in the preparation of **6** via pathway **A** do not arise from the thermodynamic point of view (possibly caused by side reactions). Since the anionic compounds [$EPh_2BH_2EPh_2$]$^-$ are isoelectronic to the well-known neutral 1,1-bis(diphenylphosphino)methane (dppm) and 1,1-bis(diphenylarsino)methane (dpam), it is of interest to compare their donor properties. BH_3 was chosen as a model Lewis acid. Reactions with BH_3NMe_3 are slightly endergonic for dppm and dpam, but exergonic for their anionic boron-containing analogs [$PPh_2BH_2PPh_2$]$^-$ and [$AsPh_2BH_2AsPh_2$]$^-$. Expectedly, mono *tert*-butyl-substituted compounds are more basic than the diphenyl derivatives. The donor properties of all studied compounds with respect to BH_3 (standard dissociation enthalpies of complexes, in kJ mol^{-1}) increase in the order: dpam (85) < dppm (116) < [$AsPh_2BH_2AsPh_2$]$^-$ (128) < [AsH_2BH_2AsH(^{t}Bu)]$^-$ (137) < [PH_2BH_2AsH(^{t}Bu)]$^-$ (139) < [$PPh_2BH_2PPh_2$]$^-$ (147) < [AsH_2BH_2PH(^{t}Bu)]$^-$ (165) < [PH_2BH_2PH(^{t}Bu)]$^-$ (167). Thus, the new anionic analogs of dpam and dppm presented in this work have stronger donor properties than their organic derivatives and might be suitable as perspective ligands in coordination chemistry.

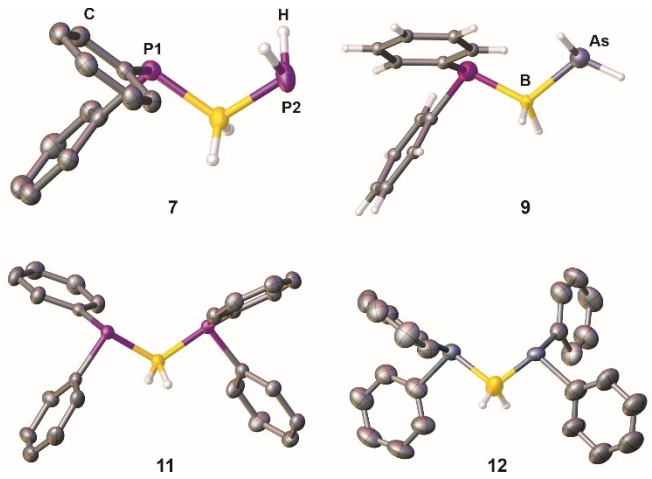

Figure 2. Molecular structures of the anions in **7**, **9**, **11** and **12**. Hydrogen atoms bonded to carbon atoms as well as cations are omitted for clarity (not for **9**). Thermal ellipsoids are drawn with 50% probability, except for **9** which is depicted in the ball and stick model.[22] In case of disorder, only the major part is depicted.

The synthesis of the three-membered anionic compounds **3**–**5** and **7**–**10** from the reaction of the pnictogenylboranes H_2E–BH_2·NMe_3 **2a** and **2b** with substituted pnictogenide salts **1a**–**1d** reveals a substitution of NMe_3 by [ER1R2]$^-$ groups. This process led to the question of whether it is possible to involve the obtained anionic three-membered salts in reactions with the pnictogenylboranes H_2E–BH_2·NMe_3 **2a** and **2b** in order to obtain longer chains of such anionic derivatives. Accordingly, compounds **3**, **7** and **9′** ([Na(18-crown-6)][H_2As–BH_2–PPh_2]) were prepared "in situ" from the reaction of the corresponding starting materials and by adding equimolar amounts of H_2E–BH_2–NMe_3 (E = P, As) to their solutions. These reactions allowed the formation of the novel five-membered anionic derivatives **13**–**16** in moderate to excellent yields (Scheme 2). Sonication of **7** and **9′** with one equivalent of **2a** and **2b**, respectively, leads to the synthesis of compounds **14** and **15**. Stirring solutions of **7** and **3** with one equivalent of H_2As–BH_2–NMe_3 (**2b**) at room temperature is sufficient for the formation of compounds **16** and **13** (Scheme 2).

According to heteronuclear NMR spectroscopy of the crude reaction solutions, compounds **14**–**16** are generated very selectively. During the synthesis of **13**, the formation of minor side products can be observed. The ^{31}P NMR spectra of the isolated products reveal that, compared to their three-membered precursors **3**, **7** and **9′**, the signals attributed to the PPh_2 group of the compounds **14**–**16** are shifted to a lower field by approximately 16 ppm. In case of the *tert*-butyl-substituted derivative **13**, the observed low field shift is more accentuated (40 ppm).

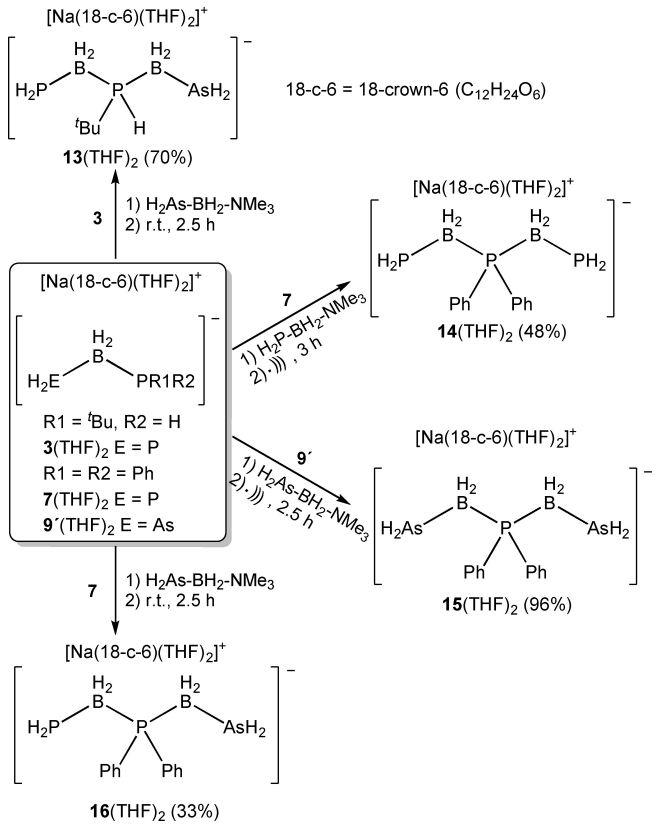

Scheme 2. Reaction of the three-membered substituted chain-like compounds **3**, **7** and **9′** with Lewis base-stabilized pnictogenylboranes **2a** and **2b**. Formation of the five-membered substituted chain-like compounds **13–16**. Isolated yields are given in parentheses. 18-c-6 = 18-crown-6 ($C_{12}H_{24}O_6$).

Reactions of **3**, **7** and **9′** with equimolar amounts of H_2E–BH_2–NMe_3 (E = P, As) lead to the substitution of NMe_3 under the formation of a new phosphorus-boron bond. Due to this new bond, the electron density of the centered phosphorus atom is lowered resulting in the observed low field shift of the corresponding signal. Contrary to the shift of the signal attributed to the central substituted phosphine, the signals of the terminal PH_2 groups of **14** and **16** are shifted to a higher field (by approximately 16 and 18 ppm, respectively) in comparison to starting material **7**. The signal corresponding to the PH_2 group of **13** reveals a slightly reduced shift (approximately 14 ppm) as compared to compounds **14** and **16**. In the ^{11}B NMR spectra for all products, a low field shift of the signals related to the BH_2 groups are detected (Table 2).

In the ^{1}H NMR spectra of **14** and **16**, signals attributed to the PH_2 groups are found at approximately 0.74 ppm as broad doublets with similar coupling constants (**14**: $^1J_{H,P}$ = 181 Hz, **16**: $^1J_{H,P}$ = 179 Hz). The signals corresponding to the AsH_2 groups of **15** and **16** are observed at approximately −0.21 ppm indicating a hydridic character. The signals attributed to the BH_2 groups of **14** and **15** are detected at slightly different chemical shifts (**14**: 1.51 ppm, **15**: 1.65 ppm). This difference is probably assigned to the different terminal substituents in **14** (PH_2) and **15** (AsH_2). Compound **16** shows two signals for the BH_2 groups (1.51 ppm and 1.63 ppm) as expected because it is composed of two different BH_2 moieties. Unsurprisingly, the shifts of these signals are similar to those found for the BH_2 groups in **14** and **15** thanks to the presence of both terminal PH_2 and AsH_2 groups in **16**. Due to the chirality in compound **13**, two sets of signals are observed in its ^{1}H NMR spectrum indicating the presence of two isomers in solution. The signal ascribed to the PH_2 group in **13** exists as two broad doublets with a slight downfield shift compared to those of **14** and **16** (**13**: 0.9 and 1.03 ppm, **14**: 0.74 ppm, **16**: 0.75 ppm). Additionally, two multiplets are observed for the AsH_2 group in **13** which are as well downfield shifted compared to **15** and **16** (**13**: 0.00 ppm, **15**: −0.20 ppm, **16**: −0.22 ppm). For the two signals attributed to the BH_2 groups of **13**, a slight upfield shift is detected (signals located at 1.1 ppm) compared to **14–16**.

Single crystals suitable for X-ray diffraction experiments are obtained for all those compounds by storing a saturated THF/*n*-hexane solution (**14**), saturated THF solution (**15**) and THF solutions layered with *n*-hexane (**16**, **13**) at −28 °C. The solid-state structures of the anionic parts of compounds **13–16** are shown in Figure 3. Compound **13** crystalizes in the centrosymmetric space group *C*2/c. In the solid-state structure, two isomers *R:S* with a 50:50 ratio are observed. In Figure 3, only the *R* isomer is shown. The determined geometrical parameters including the bond lengths and angles of **14–16** are very similar to those of **7**. Compared to **3** as well as to compounds **14–16**, in **13**, a shorter distance between the terminal phosphanyl group and the neighboring BH_2 group (P–B 2.001(2) Å) as well as the terminal arsanyl group and its neighboring BH_2 group (As–B 2.034(1) Å) is observed. Additionally, the P–B–P angle in **13** is wider by approximately 6° and the As–B–P angle is comparable to the values of **9**, **15** and **16** (for further data see Supporting Information). The solid-state structure of compounds **14–16** reveal an antiperiplanar conformation of the pnictogen atom lone pair and the backbone of the molecule for the EH_2–BH_2 fragment (E = P, As). Additionally, a synclinal

Table 2. NMR data of compounds **13–16** compared to **3**, **7** and **9′**; $[H_2P^b$–B^cH_2–P^aR1R2–B^dH_2–$AsH_2]^-$; **A**: R1 = R2 = Ph; **B**: R1 = ^{t}Bu, R2 = H.

Compound		P^aR1R2 [ppm]	P^bH_2 [ppm]	$^1J_{P,H}{}^{a/b}$ [Hz]	$B^{c/d}H_2$ [ppm]	$^1J_{B,H}{}^{c/d}$ [Hz]	$^1J_{B,P}{}^{c/d}$ [Hz]
A	**7**	−15.2	−203.3	173	−29.1/–	98	–
	9′	−16.7	–	–	−28.9/–	100	–
	14	0.1	−219.4	181	−34.4/–	–	–
	15	0.2	–	–	−34.5/–	98	69
	16	−0.6	−221.1	179	−32.3–−36.7	–	–
B	**3**	−32.9	−188.8	177/173	−33.8/–	97	27
	13	13.1	−203.4	180	−37.5/37.0	98/98	68/64

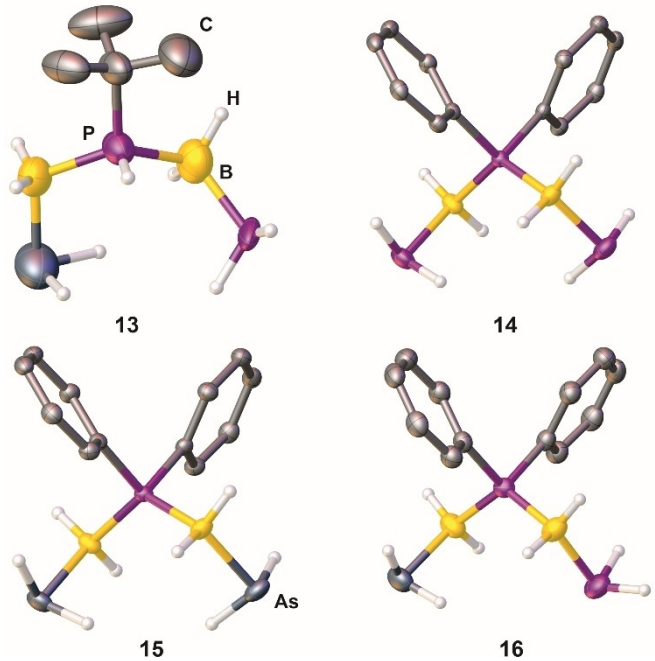

Figure 3. Molecular structures of the anions in **13**–**16** in the solid state. Hydrogen atoms bonded to carbon and counter ions are omitted for clarity. Thermal ellipsoids are drawn with 50% probability. In case of disorder, only the major part is depicted.

arrangement of EH_2 and the BH_2–EH_2 groups (E = P, As) is observed for the BH_2–PPh_2 fragment.

In the ESI–MS (anion mode) spectra, the molecular ion peak corresponding to the anion for each compound is detected. Sonication or heating of **3** with one equivalent of Lewis base-stabilized phosphanylborane does not lead to the desired product $[H_2P–BH_2–^tBuPH–BH_2–PH_2]^-$. According to the ^{31}P NMR spectrum of the reaction mixture only the formation of side and decomposition products could be observed. Despite using various purification methods, the identification or isolation of the reaction products were not successful. The experimental approach proves that for the formation of **13** stirring of $H_2As–BH_2–NMe_3$ with **3** at room temperature is sufficient. Under the same reaction conditions, no reaction can be observed with the Lewis base-stabilized phosphanylborane. In order to gain a deeper insight into the different reactivities of the phosphorus and arsenic derivatives, DFT computations were performed. The gas phase reactions of $[PH_2BH_2PH^tBu]^-$ both with $PH_2BH_2NMe_3$ and $AsH_2BH_2NMe_3$ are exothermic and exergonic by circa 55 kJ mol^{-1} (see Supporting Information for details). Thus, the formation of $[PH_2BH_2PH^tBuBH_2PH_2]^-$ is as thermodynamically favorable as $[PH_2BH_2PH^tBuBH_2AsH_2]^-$. NMe_3 elimination with B–N bond breaking in $PH_2BH_2NMe_3$ is by 14 kJ mol^{-1} less energetically demanding as compared to its arsenic derivative, which may facilitate side reactions of monomeric PH_2BH_2 unit.

Conclusion

Reacting Lewis base-stabilized pnictogenylboranes with substituted pnictogenide salts leads to the novel three-membered anionic chain-like compounds **3**–**10** in good yields. Depending on the combination of the starting materials, not only phosphorus- or arsenic-containing compounds but also derivatives containing both pnictogen atoms are easily accessible that way. Additionally, the synthesis of the first 1,1-bis(diphenylphosphino)borate (**11**) and 1,1-bis(diphenylarsino)borate (**12**) are presented. Compounds **11** and **12** are isostructural to dppm (1,1-bis(diphenylphosphino)methane) and dpam (1,1-bis(diphenylarsino)methane), but reveal stronger donor abilities as computations show. As negatively charged inorganic analogs of these established ligands, compounds **11** and **12** are promising alternatives offering different reactivities/properties.

Furthermore, a simple synthetic route is shown to obtain organosubstituted five-membered oligomers with alternating group 13/15 elements. Beside $[Na(18\text{-crown-}6)][H_2P–BH_2–Ph_2P–BH_2–PH_2]$ (**14**) revealing a pure phosphorus boron backbone, similar compounds are accessible bearing one (**16**, **13**) or two (**15**) terminal arsanyl groups. Due to the presence of two coordination sites in the form of phosphine and arsine groups, compounds **3**, **4**, **7**–**16** are interesting candidates for a future coordination chemistry with their coordination behavior already being in the focus of current investigations. Finally, it is worth mentioning that compounds **3**–**16** are extremely sensitive, decompose easily and in corresponding reactions they are very hard to handle. Thus, for each compound several attempts were made in order to optimize the experimental conditions for its synthesis and to obtain the highest yields.

Experimental Section

Apparatus, materials and methods: All manipulations were performed under an atmosphere of dry argon/ nitrogen using standard glove-box and Schlenk techniques. All solvents were degassed and purified by standard procedures. The compounds $H_2E–BH_2–NMe_3$ (E = P, As),[13c] $KAsPh_2$,[24] $NaPPh_2$,[10b] Na^tBuPH[10c] and Na^tBuAsH[17] were prepared according to literature procedures. Other chemicals were obtained from STREM Chemicals, INC. (PPh_2H). The NMR spectra were recorded either on an Avance 400 spectrometer (**3**–**16**) (^1H: 400.13 MHz, ^{31}P: 161.976 MHz, ^{11}B: 128.378 MHz, $^{13}C\{^1H\}$: 100.623 MHz) with δ [ppm] referenced to external $SiMe_4$ (^1H, ^{13}C), H_3PO_4 (^{31}P), $BF_3 \cdot Et_2O$ (^{11}B) or an Avance III HD 600 spectrometer (**4**) (^1H: 600.13 MHz). IR spectra were recorded either on a DIGILAB (FTS 800) FT IR spectrometer (**3**, **5**, **6**, **7**, **8**, **14**, **15**) or a Thermo Scientific (NICOLET iS 5, iD1 Transmission) FT IR spectrometer (**4**, **9**, **10**, **11**, **12**, **13**, **16**) with $\tilde{\nu}$ [cm^{-1}]. Mass spectra were recorded either on a ThermoQuest Finnigan TSQ 7000 (**3**, **7**, **14**, **15**; Mass-Spectrometry-Department, University of Regensburg) or a Waters/Micromass LCT-TOF classic (**4**, **5**, **6**, **8**, **9**, **10**, **11**, **12**, **13**, **16**; Mass Spectrometer in the Working group) (Supporting Information-MS). The C, H, N analyses were measured on an Elementar Vario EL III apparatus (**3**–**16**). C, H, N analyses were carried out repeatedly. Different amounts of coordinating THF have been found in nearly all cases. Total removal of the THF was not always possible, however, the C, H, N analyses are in good

agreement with the expected values considering a varying THF-content (0.5% tolerance).

Experimental details

Synthesis of $[Na(C_{12}H_{24}O_6)(THF)_2][H_2P{-}BH_2{-}^tBuPH]$ (3(THF)$_2$): A solution of 106 mg (1.00 mmol) $H_2P{-}BH_2{-}NMe_3$ in 2 mL toluene is added to a solution of 112 mg (1.00 mmol) Na^{t}BuPH in 20 ml THF at room temperature. The reaction mixture is sonicated for 2.5 h after which the solution is filtered onto 264 mg (1.00 mmol) solid $C_{12}H_{24}O_6$ (18-crown-6). The solution is layered with 60 mL of *n*-hexane. **3**(THF)$_2$ crystallizes at 4 °C as colorless blocks. The supernatant is decanted, the crystals are separated, washed with cold *n*-hexane (0 °C, 3×5 mL) and dried *in vacuo*. Yield (**3**(THF)$_{0.15}$): 374 mg (86%).

Synthesis of $[Na(C_{12}H_{24}O_6)(THF)_2][H_2As{-}BH_2{-}^tBuAsH]$ (4(THF)$_2$): A solution of 79 mg (0.50 mmol) $H_2As{-}BH_2{-}NMe_3$ in 1 ml toluene is added to a solution of 78 mg (0.50 mmol) Na^{t}BuAsH in 5 ml THF at room temperature and stirred for 16 h. The solution is filtered onto 125 mg (0.47 mmol) solid $C_{12}H_{24}O_6$ (18-crown-6) and layered with 25 ml *n*-hexane. **4**(THF)$_2$ crystallizes at −28 °C as colorless blocks. The supernatant is decanted, the crystals are separated, washed with cold *n*-hexane (−30 °C, 3×10 ml) and dried *in vacuo*. Yield (**4**(THF)$_{0.75}$): 186 mg (71%).

Synthesis of $[Na(C_{12}H_{24}O_6)(THF)_2][H_2P{-}BH_2{-}^tBuAsH]$ (5(THF)$_2$): A solution of 52 mg (0.50 mmol) $H_2P{-}BH_2{-}NMe_3$ in 1 ml toluene is added to a solution of 78 mg (0.50 mmol) Na^{t}BuAsH in 5 ml THF at room temperature and stirred for 16 h. The solution is filtered onto 127 mg (0.48 mmol) solid $C_{12}H_{24}O_6$ (18-crown-6) and layered with 20 ml of *n*-hexane. **5**(THF)$_2$ crystallizes at −28 °C as colorless blocks. The supernatant is decanted, the crystals are separated, washed with cold *n*-hexane (−30 °C, 2×10 ml) and dried *in vacuo*. Yield (**5**(THF)$_{0.2}$): 150 mg (65%).

Synthesis of $[Na(C_{12}H_{24}O_6)(THF)_2][H_2As{-}BH_2{-}^tBuPH{-}BH_3]$ (6(THF)$_2$): 150 mg (1.00 mmol) $H_2As{-}BH_2{-}NMe_3$ in 1 ml toluene are added to a solution of 115 mg (0.91 mmol) Na[^{t}BuPH–BH_3] and stirred for 16 h at room temperature. The solution is filtered onto 225 mg (0.85 mmol) $C_{12}H_{24}O_6$ and all volatiles are removed *in vacuo*. The residue is dissolved in 4 ml THF and layered with 20 ml of *n*-hexane. **6**(THF)$_2$ crystallizes at −30 °C as colorless blocks. The supernatant is decanted, the crystals are separated, washed with cold *n*-hexane (−30 °C, 2×5 ml) and dried *in vacuo*. **6**(THF)$_2$ is an oil at room temperature. The formation of Na[$H_3B{-}^t$BuPH–BH_3] as a side product can be observed by ^{31}P NMR spectroscopy. Yield (**6**(THF)$_n$): 237 mg (58%).

Synthesis of $[Na(C_{12}H_{24}O_6)(THF)_2][H_2P{-}BH_2{-}PPh_2]$ (7(THF)$_2$): A solution of 106 mg (1.00 mmol) $H_2P{-}BH_2{-}NMe_3$ in 2 mL toluene is added to a solution of 208 mg (1.00 mmol) $NaPPh_2$ in 20 ml THF. The mixture is sonicated for 2.5 h after which it is filtered onto 264 mg (1.00 mmol) solid $C_{12}H_{24}O_6$ (18-crown-6). After the removal of all volatiles *in vacuo*, **7** is dissolved in 5 mL THF and filtered again. The solvent is removed *in vacuo* and 20 mL *n*-hexane are added to the white solid. THF is added dropwise until a clear colorless solution is obtained. **7**(THF)$_2$ crystallizes at −28 °C as colorless blocks. The supernatant is decanted, the crystals are separated, washed with cold *n*-hexane (0 °C, 3×5 mL) and dried *in vacuo*. **7**(THF)$_2$ is a colorless waxy solid/oil at room temperature. Yield (**7**(THF)$_{1.1}$): 310 mg (52%).

Synthesis of $[K(C_{18}H_{36}N_2O_6)][H_2As{-}BH_2{-}AsPh_2]$ (8): A solution of 75 mg (0.50 mmol) $H_2As{-}BH_2{-}NMe_3$ in 1 ml toluene is added to a solution of 156 mg (0.50 mmol) $KAsPh_2(C_4H_8O_2)_{0.625}$ in 5 ml THF and is stirred for 16 h at 60 °C. The reaction mixture is filtered on 170 mg (0.45 mmol) solid $C_{18}H_{26}N_2O_6$ ([2.2.2]cryptand) and layered with 25 ml of diethyl ether. **8** crystallizes at −28 °C as thin orange plates. The supernatant is decanted, the crystals are separated, washed with cold diethyl ether (−30 °C, 3×5 ml) and dried *in vacuo*. Yield (**8**): 233 mg (63%).

Synthesis of $[Na(C_{18}H_{36}N_2O_6)][H_2As{-}BH_2{-}PPh_2]$ (9): A solution of 177 mg (1.0 mmol) $NaPPh_2$ in 1 ml THF is added to a solution of 148 mg (1.0 mmol) $H_2As{-}BH_2{-}NMe_3$ in 4 ml THF. After stirring for 16 h at room temperature, the reaction solution is filtered onto 339 mg (0.9 mmol) solid $C_{18}H_{36}N_2O_6$ ([2.2.2]cryptand). The obtained solution is layered with 20 ml diethyl ether. **9** crystallizes at −30 °C as colorless blocks. The supernatant is decanted, the crystals are separated, washed with cold diethyl ether (−30 °C, 2×10 ml) and dried *in vacuo*. Yield (**9**): 368 mg (61%).

Synthesis of $[K(C_{18}N_2H_{36}O_6)][H_2P{-}BH_2{-}AsPh_2]$ (10): A solution of 105 mg (1.00 mmol) $H_2P{-}BH_2{-}NMe_3$ in 2 ml toluene is added to a solution of 323 mg (1.00 mmol) $KAsPh_2(C_4H_8O_2)_{0.625}$ in 4 ml THF and stirred for 16 h at 70 °C. The reaction solution is filtered on 370 mg (0.98 mmol) solid $C_{18}N_2H_{36}O_6$ ([2.2.2]cryptand) and layered with 25 ml diethyl ether. **10** crystallizes at −28 °C as thin red plates. The supernatant is decanted, the crystals are separated, washed with cold diethyl ether (−30 °C, 3×5 ml) and dried *in vacuo*. Yield (**10**): 481 mg (71%).

Synthesis of $[Na(C_{12}H_{24}O_6)(THF)_2][Ph_2P{-}BH_2{-}PPh_2]$ (11(THF)$_2$): A solution of 202 mg (1.00 mmol) $IBH_2{-}SMe_2$ in 1 ml toluene is added to a solution of 410 mg (2.00 mmol) $NaPPh_2$ in 8 ml THF at −80 °C. The solution is stirred for 16 h while being allowed to reach room temperature. The yellow reaction solution is filtered on 185 mg (0.70 mmol) solid $C_{12}H_{24}O_6$ (18-crown-6) and layered with 25 ml diethyl ether. **11**(THF)$_2$ crystallizes at −30 °C as colorless blocks. The supernatant is decanted, the crystals are separated, washed with cold diethyl ether (−30 °C, 2×5 ml) and dried *in vacuo*. Yield (**11**(NaI)$_{0.07}$): 405 mg (85%).

Synthesis of $[K(C_{12}H_{24}O_6)(THF)_2][Ph_2As{-}BH_2{-}AsPh_2]$ (12(THF)$_2$): A solution of 100 mg (0.50 mmol) $IBH_2{-}SMe_2$ in 1 ml toluene is added to a solution of 326 mg (1.00 mmol) $KAsPh_2{\cdot}(C_4H_8O_2)_{0.625}$ in 5 ml THF at −80 °C. The solution is stirred for 16 h while allowed to reach room temperature. The reaction mixture is filtered on 264 mg (1.00 mmol) solid $C_{12}H_{24}O_6$ (18-crown-6) and layered with 30 ml diethyl ether. **12**(THF)$_2$ crystallizes at −30 °C as colorless blocks. The supernatant is decanted, the crystals are separated, washed with cold diethyl ether (−30 °C, 2×4 ml) and dried *in vacuo*. Yield (**12**): 302 mg (78%).

Synthesis of $[Na(C_{12}H_{24}O_6)(THF)_2][H_2P{-}BH_2{-}^tBuPH{-}BH_2{-}AsH_2]$ (13(THF)$_2$): A solution of 104 mg (0.70 mmol) $H_2As{-}BH_2{-}NMe_3$ in 1 ml toluene is added to a solution of 295 mg (0.70 mmol) [Na(18-crown-6)][$H_2P{-}BH_2{-}^t$BPH] (**3**) in 8 ml THF. The reaction mixture is stirred for 16 h at room temperature, the solution is filtered and layered with 20 mL of *n*-hexane. **13**(THF)$_2$ crystallizes at −30 °C as brown blocks. The supernatant is decanted, the remaining crystals are washed with cold *n*-hexane (−30 °C, 2×5 ml) and dried *in vacuo*. **13** is an oil at room temperature. Yield (**13**): 252 mg (70%).

Synthesis of $[Na(C_{12}H_{24}O_6)(THF)_2][H_2P{-}BH_2{-}Ph_2P{-}BH_2\text{-}PH_2]$ (14(THF)$_2$): A solution of 27 mg (0.25 mmol) $H_2PBH_2{\cdot}NMe_3$ in 0.5 mL toluene is added to a solution of 130 mg (0.25 mmol) [Na-($C_{12}H_{24}O_6$)][$H_2P{-}BH_2{-}PPh_2$] (**7**) in 8 ml THF. After sonication of the mixture for 3 h, the solution is filtered and all volatiles are removed under reduced pressure. The remaining solid is dissolved in 5 mL of THF and filtered again. The solvent is removed and 20 mL of *n*-hexane are added to the white solid. THF is added dropwise until a clear colorless solution is obtained. **14**(THF)$_2$ crystallizes at −28 °C as colorless plates. The supernatant is decanted, the remaining crystals are washed with cold *n*-hexane (0 °C, 3×5 mL) and dried *in vacuo*. Yield (**14**): 70 mg (48%).

Synthesis of $[Na(C_{12}H_{24}O_6)(THF)_2][H_2As{-}BH_2{-}Ph_2P{-}BH_2{-}AsH_2]$ (15(THF)$_2$): A solution of 521 mg (3.5 mmol) $H_2As{-}BH_2{\cdot}NMe_3$ in 3.5 mL toluene is added to a solution of 1.124 g (2.0 mmol) $[Na(C_{12}O_6H_{24})][H_2As{-}BH_2{-}PPh_2]$ (**9'**) in 10 mL THF. After sonication of the mixture for 2.5 h, the colorless solution is filtered. After concentration **15**$(THF)_2$ crystallizes at −30 °C as colorless blocks. The supernatant is decanted, the remaining crystals are washed with cold *n*-hexane (−30 °C, 7×5 mL) and dried *in vacuo*. Yield (**15**$(THF)_{0.45}$): 1.320 g (96 %).

Synthesis of $[Na(C_{12}H_{24}O_6)(THF)_2][H_2P{-}BH_2{-}Ph_2P{-}BH_2{-}AsH_2]$ (16(THF)$_2$): A solution of 75 mg (0.50 mmol) $H_2As{-}BH_2{-}NMe_3$ in 1 ml toluene is added to a solution of 130 mg (0.25 mmol) $[Na(C_{12}H_{24}O_6)][H_2P{-}BH_2{-}PPh_2]$ (**7**) in 8 ml THF and stirred for 16 h at room temperature. The reaction liquid is filtered and layered with 25 ml of *n*-hexane. **16**$(THF)_2$ crystallizes at −30 °C as colorless blocks. The supernatant is decanted, the remaining crystals are washed with cold *n*-hexane (−30 °C, 2×5 ml) and dried *in vacuo*. Yield (**16**$(THF)_{0.2}$): 104 mg (33 %).

DFT calculations: For all computations, the Gaussian 09 program package[25] was used throughout. Density functional theory (DFT) in the form of Becke's three-parameter hybrid functional B3LYP[26] with a 6-311++G** all-electron basis set was employed. The geometries of the compounds were fully optimized and verified to be true minima on their respective potential energy surface.

Crystallographic data: Deposition Number(s) 2207469 (**3**), 2207470 (**4**), 2207471(**6**), 2207472 (**7**), 2207473 (**11**), 2207474 (**12**), 2207475 (**13**), 2207476 (**14**), 2207477 (**15**) and 2207478 (**16**) contain(s) the supplementary crystallographic data for this paper. These data are provided free of charge by the joint Cambridge Crystallographic Data Centre and Fachinformationszentrum Karlsruhe Access Structures service.

Acknowledgements

This work was supported by the joint DFG-RSF project (DFG Sche 384/41-1 and RSF grant 21-43-04404). Computational resources of the research center "Computing Center" of the research park of St. Petersburg State University were used. Open Access funding enabled and organized by Projekt DEAL.

Conflict of Interest

The authors declare no conflict of interest.

Data Availability Statement

The data that support the findings of this study are available in the supplementary material of this article.

Keywords: anionic chains · arsenic · boron · NMR spectroscopy · phosphorus

[1] a) G. Onodera, H. Kumagae, D. Nakamura, T. Hayasaki, T. Fukuda, M. Kimura, *Tetrahedron Lett.* **2020**, *61*, 152537; b) L. J. Morris, M. S. Hill, M. F. Mahon, I. Manners, B. O. Patrick, *Organometallics* **2020**, *39*, 4195–4207; c) G. Bas de Jong, N. Ortega, M. Lutz, K. Lammertsma, J. C. Slootweg, *Chem. Eur. J.* **2020**, *26*, 15944–15952; d) C. Alayrac, S. Lakhdar, I. Abdellah, A.-C. Gaumont, *Top. Curr. Chem.* **2014**, *361*, 1–82; e) A. Amgoune, G. Bouhadir, D. Bourissou, *Top. Curr. Chem.* **2013**, *334*, 281–312; f) G. B. Consiglio, P. Queval, A. Harrison-Marchand, A. Mordini, J.-F. Lohier, O. Delacroix, A.-C. Gaumont, H. Gérard, J. Maddaluno, H. Oulyadi, *J. Am. Chem. Soc.* **2011**, *133*, 6472–6480; g) S. J. Geier, T. M. Gilbert, D. W. Stephan, *Inorg. Chem.* **2011**, *50*, 336–344; h) A. Staubitz, A. P. M. Robertson, M. E. Sloan, I. Manners, *Chem. Rev.* **2010**, *110*, 4023–4078.

[2] a) S. Lemouzy, R. Membrat, E. Oliviere, M. Jean, M. Albalat, D. Nuel, L. Giordano, D. Hérault, G. Buono, *J. Org. Chem.* **2019**, *84 (7)*, 4551–4557; b) S. Konishi, T. Iwai, M. Sawamura, *Organometallics* **2018**, *37*, 1876–1883; c) M. Dutartre, J. Bayardon, S. Jugé, *Chem. Soc. Rev.* **2016**, *45*, 5771–5794; d) T. Imamoto, K. Tamura, Z. Zhang, Y. Horiuchi, M. Sugiya, K. Yoshida, A. Yanagisawa, I. D. Grindnev, *J. Am. Chem. Soc.* **2012**, *134*, 1754–1769.

[3] a) R. Declercq, G. Bouhadir, D. Bourissou, M.-A. Légaré, M.-A. Courtemanche, K. S. Nahi, N. Bouchard, F.-G. Fontaine, L. Maron, *ACS Catal.* **2015**, *5*, 2513–2520; b) M.-A. Courtemanche, M.-A. Légaré, L. Maron, F.-G. Fontaine, *J. Am. Chem. Soc.* **2014**, *136*, 10708–10717.

[4] Selected articles: a) A. W. Knights, S. S. Chitnis, I. Manners, *Chem. Sci.* **2019**, *10*, 7281–7289; b) C. A. Busacca, J. A. Milligan, E. Rattanangkool, C. Ramavarapu, A. Chen, A. K. Saha, Z. Li, H. Lee, S. J. Geib, G. Wang, C. H. Senanayake, P. Wipf, *J. Org. Chem.* **2014**, *79*, 9878–9887 (and references cited therein); c) C. A. Busacca, B. Qu, E. Farber, N. Haddad, N. Grět, A. K. Saha, M. C. Eriksson, J.-P. Wu, K. R. Fandrick, S. Han, N. Grinberg, S. Ma, H. Lee, Z. Li, M. Spinelli, A. Gold, Z. Wang, G. Wang, P. Wipf, C. H. Senanayake, *Org. Lett.* **2013**, *15*, 1136–1139; d) C. A. Busacca, B. Qu, E. Farber, N. Haddad, N. Grět, A. K. Saha, M. C. Eriksson, J.-P. Wu, K. R. Fandrick, S. Han, N. Grinberg, S. Ma, H. Lee, Z. Li, M. Spinelle, A. Gold, G. Wang, P. Wipf, C. H. Senanayake, *Org. Lett.* **2013**, *15*, 1132–1135.

[5] a) D. A. Janus, C. J. Lieven, M. E. Crowe, L. A. Levin, *Pharm. Dev. Technol.* **2018**, *23*, 882–889; b) N. J. Niemuth, A. F. Thompson, M. E. Crowe, C. J. Lieven, L. A. Levin, *Neurochem. Int.* **2016**, *99*, 24–32; c) M. E. Crowe, C. J. Lieven, A. F. Thompson, N. Sheibani, L. A. Levin, *Redox Biol.* **2015**, *6*, 73–79.

[6] Selected articles: a) J. H. W. LaFortune, Z.-W. Qu, K. L. Bamford, A. Trofimova, S. A. Westcott, D. W. Stephan, *Chem. Eur. J.* **2019**, *25*, 12063–12067; b) N. Szynkiewicz, A. Ordyszewska, J. Chojnacki, R. Grubba, *RSC Adv.* **2019**, *9*, 27749–27753; c) M.-A. Courtemanche, M.-A. Légaré, L. Maron, F.-G. Fontaine, *J. Am. Chem. Soc.* **2013**, *135*, 9326–9329; d) S. J. Geier, T. M. Gilbert, D. W. Stephan, *Inorg. Chem.* **2011**, *50*, 336; e) S. J. Geier, T. M. Gilbert, D. W. Stephan, *J. Am. Chem. Soc.* **2008**, *130*, 12632–12633; f) G. C. Welch, R. R. S. Juan, J. D. Masuda, D. W. Stephan, *Science* **2006**, *314*, 1124–1126.

[7] a) J. R. Turner, D. A. Resendiz-Lara, T. Jurca, A. Schäfer, J. R. Vance, L. Beckett, G. R. Whittell, R. A. Musgrave, H. A. Sparkes, I. Manners, *Macromol. Chem. Phys.* **2017**, *218*, 1700120; b) A. Schäfer, T. Jurca, J. Turner, J. R. Vance, K. Lee, V. A. Du, M. F. Haddow, G. R. Whittell, I. Manners, *Angew. Chem. Int. Ed.* **2015**, *54*, 4836–4841; *Angew. Chem.* **2015**, *127*, 4918–4923; c) S. Pandey, P. Lönnecke, E. Hey-Hawkins, *Eur. J. Inorg. Chem.* **2014**, 2456–2465; d) T. L. Clark, J. M. Rodezno, S. B. Clendenning, S. Aouba, P. M. Brodersen, A. J. Lough, H. E. Ruda, I. Manners, *Chem. Eur. J.* **2005**, *11*, 4526–4534; e) H. Dorn, J. M. Rodenzo, B. Brunnhöfer, E. Rivard, J. A. Massey, I. Manners, *Macromolecules* **2003**, *36*, 291–297; f) A. B. Burg, R. I. Wagner, *J. Am. Chem. Soc.* **1953**, *75*, 3872–3877.

[8] a) D. Han, F. Anke, M. Trose, T. Beweries, *Coord. Chem. Rev.* **2019**, *380*, 260; b) J. A. Bailey, P. G. Pringle, *Coord. Chem. Rev.* **2015**, *297 (298)*, 77; c) R. T. Paine, H. Nöth, *Chem. Rev.* **1995**, *95*, 343.

[9] a) D. A. Resendiz-Lara, V. T. Annibale, A. W. Knights, S. S. Chitnis, I. Manners, *Macromolecules* **2021**, *54*, 71–82; b) A. W. Knights, S. S. Chitnis, I. Manners, *Chem. Sci.* **2019**, *10*, 7281–7289; c) U. S. D. Paul, H. Braunschweig, U. Radius, *Chem. Commun.* **2016**, *52*, 8573–8576; d) F. Schön, L. M. Sigmund, F. Schneider, D. Hartmann, M. A. Wiebe, I. Manners, L. Greb, *Angew. Chem. Int. Ed.* **2022**, *61*, e202202176.

[10] a) N. L. Oldroyd, S. S. Chitnis, V. T. Annibale, M. I. Arz, H. A. Sparkes, I. Manners, *Nat. Commun.* **2019**, *10*, 1370; b) A. Stauber, T. Jurca, C. Marquardt, M. Fleischmann, M. Seidl, G. R. Whittell, I. Manners, M. Scheer, *Eur. J. Inorg. Chem.* **2016**, 2684–2687; c) C. Marquardt, T. Jurca, K.-C. Schwan, A. Stauber, A. V. Virovets, G. R. Whittell, I. Manners, M. Scheer, *Angew. Chem. Int. Ed.* **2015**, *54*, 13782–13786; *Angew. Chem.* **2015**, *127*, 13986–13991.

[11] a) C. Marquardt, A. Adolf, A. Stauber, M. Bodensteiner, A. V. Virovets, A. Timoshkin, M. Scheer, *Angew. Chem. Int. Ed.* **2013**, *19*, 11887–11891; b) K.-C. Schwan, A. Timoshkin, M. Zabel, M. Scheer, *Angew. Chem. Int. Ed.* **2006**, *12*, 4900–4908.

[12] a) M. Elsayed Moussa, C. Marquardt, O. Hegen, M. Seidl, M. Scheer, *New J. Chem.* **2021**, *45*, 14916–14919; b) M. Elsayed Moussa, J. Braese, C. Marquardt, M. Seidl, M. Scheer, *Eur. J. Inorg. Chem.* **2020**, *26*, 2501–2505; c) J. Braese, A. Schinabeck, M. Bodensteiner, H. Yersin, A. Y. Timoshkin, M. Scheer, *Chem. Eur. J.* **2018**, *24*, 10073–10077.
[13] a) C. Marquardt, T. Kahoun, J. Baumann, A. Y. Timoshkin, M. Scheer, *Z. Anorg. Allg. Chem.* **2017**, *643*, 1326–1330; b) C. Marquardt, O. Hegen, T. Kahoun, M. Scheer, *Chem. Eur. J.* **2017**, *23*, 4397–4404; c) C. Marquardt, A. Adolf, A. Stauber, M. Bodensteiner, A. V. Virovets, A. Y. Timoshkin, M. Scheer, *Chem. Eur. J.* **2013**, *19*, 11887–11891; d) A. Adolf, M. Zabel, M. Scheer, *Eur. J. Inorg. Chem.* **2007**, 2136–2143; e) K.-C. Schwan, A. Y. Timoskin, M. Zabel, M. Scheer, *Chem. Eur. J.* **2006**, *12*, 4900–4908.
[14] a) C. Marquardt, G. Balázs, J. Baumann, A. V. Virovets, M. Scheer, *Chem. Eur. J.* **2017**, *23*, 11423–11429; b) C. Marquardt, T. Kahoun, A. Stauber, G. Balázs, M. Bodensteiner, A. Y. Timoshkin, M. Scheer, *Angew. Chem. Int. Ed.* **2016**, *55*, 14828–14832; *Angew. Chem.* **2016**, *128*, 15048–15052; c) C. Marquardt, C. Thoms, A. Stauber, G. Balázs, M. Bodensteiner, M. Scheer, *Angew. Chem. Int. Ed.* **2014**, *53*, 3727–3730; *Angew. Chem.* **2014**, *126*, 3801–3804; d) C. Thoms, C. Marquardt, A. Y. Timoshkin, M. Bodensteiner, M. Scheer, *Angew. Chem. Int. Ed.* **2013**, *52*, 5150–5154; *Angew. Chem.* **2013**, *125*, 5254–5259.
[15] C. Marquardt, T. Jurca, K.-C. Schwan, A. Stuaber, A. V. Virovets, G. R. Whittell, I. Manners, M. Scheer, *Angew. Chem. Int. Ed.* **2015**, *54*, 13782–13786; *Angew. Chem.* **2015**, *127*, 13986–13991.
[16] C. Marquardt, T. Kahoun, A. Stauber, G. Balázs, M. Bodensteiner, A. Y. Timoshkin, M. Scheer, *Angew. Chem. Int. Ed.* **2016**, *55*, 14828–14832; *Angew. Chem.* **2016**, *128*, 15048–15052.
[17] M. Elsayed Moussa, T. Kahoun, M. T. Ackermann, M. Seidl, M. Bodensteiner, A. Y. Timoshkin, M. Scheer, *Organometallics* **2022**, *41*, 1572–1578.
[18] P. P. Power, *Angew. Chem. Int. Ed.* **1990**, *29*, 449–460; *Angew. Chem.* **1990**, *102*, 527–538.
[19] Using a Teflon-coated stirring bar turns the product color to black and the reaction solution to green. Thus, a glass-coated stirring bar is used instead. As a side product the formation of $Na[H_3B{-}^tBuPH{-}BH_3]^-$ is detected.
[20] Compounds **5** and **6** are partially contaminated with impurities ($[H_2PBH_2PH_2]^-$ and $[H_3P{-}^tBuPH{-}BH_3]^-$, respectively) of 10 to 15% depending on the sample. Due to similar solubilities of each of **5** and **6** with their associated impurities, crystals of these impurities were also found with those of **5** and **6**. Under the microscope, it is visually possible to distinguish crystals of **5** or **6** from their impurities and thus we were able to separate (in a glove box) few pure milligrams of each of them necessary for EA. However, isolation of enough pure amounts for ^{31}P or ^{11}B NMR studies was unattainable (for further information see Supporting Information).
[21] O. Hegen, A. V. Virovets, A. Y. Timoshkin, M. Scheer, *Chem. Eur. J.* **2018**, *24*, 16521–16525.
[22] The quality of the single crystals of **9** was rather low. Despite several attempts of crystallization it was not possible to receive better single crystals, and the obtained X-ray data was not sufficient for publication. Therefore, only the atom connectivity of **9** is shown and no bond distances or angles are discussed.
[23] Although the lone pair vector was not precisely evaluated, based on the molecule conformation, a sufficient qualitative estimate could be made visually.
[24] A. Tzschach, W. Lange, *Chem. Ber.* **1962**, *95*, 1360–1366. The obtained $KAsPh_2$ contains 0.625 equivalents of 1,4-dioxane.
[25] M. J. Frisch, G. W. Trucks, H. B. Schlegel, G. E. Scuseria, M. A. Robb, J. R. Cheeseman, G. Scalmani, V. Barone, B. Mennucci, G. A. Petersson, H. Nakatsuji, M. Caricato, X. Li, H. P. Hratchian, A. F. Izmaylov, J. Bloino, G. Zheng, J. L. Sonnenberg, M. Hada, M. Ehara, K. Toyota, R. Fukuda, J. Hasegawa, M. Ishida, T. Nakajima, Y. Honda, O. Kitao, H. Nakai, T. Vreven, J. A. Montgomery, Jr., J. E. Peralta, F. Ogliaro, M. Bearpark, J. J. Heyd, E. Brothers, K. N. Kudin, V. N. Staroverov, T. Keith, R. Kobayashi, J. Normand, K. Raghavachari, A. Rendell, J. C. Burant, S. S. Iyengar, J. Tomasi, M. Cossi, N. Rega, J. M. Millam, M. Klene, J. E. Knox, J. B. Cross, V. Bakken, C. Adamo, J. Jaramillo, R. Gomperts, R. E. Stratmann, O. Yazyev, A. J. Austin, R. Cammi, C. Pomelli, J. W. Ochterski, R. L. Martin, K. Morokuma, V. G. Zakrzewski, G. A. Voth, P. Salvador, J. J. Dannenberg, S. Dapprich, A. D. Daniels, O. Farkas, J. B. Foresman, J. V. Ortiz, J. Cioslowski, D. J. Fox, Gaussian 09, Revision E.01, Gaussian, Inc., Wallingford CT, **2013**.
[26] a) A. D. Becke, A new mixing of Hartree-Fock and local density-functional theories. *J. Chem. Phys.* **1993**, *98*, 1372; b) C. Lee, W. Yang, R. G Parr, Development of the Colle–Salvetti correlation-energy formula into a functional of the electron density. *Phys. Rev. B* **1988**, *37*, 785.

Manuscript received: October 13, 2022
Accepted manuscript online: December 7, 2022
Version of record online: February 20, 2023